Theory of ultrafast nonresonant multiphoton transitions in polyatomic molecules: Basics and application to optimal control theory

Volkhard May
Institut für Physik, Humboldt-Universität zu Berlin, Newtonstraße 15, D-12489 Berlin, Germany

David Ambrosek, Markus Oppel, and Leticia González
Institut für Chemie und Biochemie, Freie Universität Berlin, Takustraße 3, 14195 Berlin, Germany

A systematic approach is presented to describe nonresonant multiphoton transitions, i.e., transitions between two electronic states without the presence of additional intermediate states resonant with the single-photon energy. The method is well suited to describe femtosecond spectroscopic experiments and, in particular, attempts to achieve laser pulse control of molecular dynamics. The obtained effective time-dependent Schrödinger equation includes effective couplings to the radiation field which combine powers of the field strength and effective transition dipole operators between the initial and final states. To arrive at time-local equations our derivation combines the well-known rotating wave approximation with the approximation of slowly varying amplitudes. Under these terms, the optimal control formalism can be readily extended to also account for nonresonant multiphoton events. Exemplary, nonresonant two- and three-photon processes, similar to those occurring in the recent femtosecond pulse-shaping experiments on CpMn(CO)$_3$, are treated using related *ab initio* potential energy surfaces. © *2007 American Institute of Physics.*
[DOI: 10.1063/1.2766717]

I. INTRODUCTION

Among multiphoton transitions those excitations which take place without resonant intermediate states are of huge importance. When carrying out experiments in the strong-field regime, for example, to generate high harmonics, so-called nonresonant multiphoton transitions (NMTs) may take place. Here, by NMT it is meant that transitions between molecular energy levels (mainly electronic levels) can only take place if the energy of two or more photons induces a transition that does not involve intermediate states which support it. Consequently, NMT should appear whenever the applied frequency is at most half of the fundamental optical transition. The absence of intermediate states indicates that coupling matrix elements to the multitude of higher lying off-resonant states are very important.

NMT processes are fairly standard when considering experiments in the frequency domain. The respective theory has been worked out many years ago and is well documented in the literature[1] (see also the recent application, partly in the framework of time-dependent density functional theory[2–5]). Much less has been done, however, within the field of femtosecond spectroscopy (see Refs. 6–9). Nevertheless, NMT processes may participate in closed-loop feedback laser pulse control experiments, as those recently performed on the organometallic compound CpMn(CO)$_3$ (Cp= η^5C$_5$H$_5$).[10] The theoretical challenge of treating NMT phenomena offers a particular extension to the field of femtosecond laser pulse control of molecular dynamics (for a recent overview see Refs. 11–17). It is the aim of the present paper to achieve this by extending our preliminary considerations given in Refs. 18 and 19.

Often it suffices to describe NMT in the framework of perturbation theory with respect to the reference molecule field coupling $-\hat{\boldsymbol{\mu}}\mathbf{E}(t)$ (see Ref. 1 or the more recent works in Refs. 2–5). Here, $\hat{\boldsymbol{\mu}}$ is the molecular dipole operator and $\mathbf{E}(t)$ denotes the electric field strength of the laser pulse. Considering nonresonant two-photon processes the transition probability between the ground and the first excited state is determined by the following expression:

$$P_{g \to e} \sim \frac{E^4}{|\varepsilon_{eg} - 2\omega|^2} \left| \sum_x \frac{\langle \varphi_e | \hat{\boldsymbol{\mu}} | \varphi_x \rangle \langle \varphi_x | \hat{\boldsymbol{\mu}} | \varphi_g \rangle}{\varepsilon_{xg} - \omega} \right|^2. \quad (1)$$

The first term on the right-hand side includes the field amplitude E and indicates the possible resonant character of the two-photon transition from the ground state φ_g into the excited state φ_e (ε_{eg} is transition frequency and ω denotes the frequency of the external field). In the second term the dipole operator transition matrix elements describe transitions from the ground state into the (quasicontinuum) of high lying states φ_x and back into the first excited state. The frequency denominator indicates the nonresonant character of these transitions where the ε_{xg} denote the transition frequencies from the ground state into the off-resonant states. It is obvious that the amount of off-resonant states contributing depends on the magnitude of the overall transition probability. The used perturbational treatment of the coupling to the radiation field, however, restricts the whole description to the low-field regime.

To enter a regime of strong fields a nonperturbative incorporation of $-\hat{\boldsymbol{\mu}}\mathbf{E}(t)$ is required, which becomes possible by a direct solution of the time-dependent Schrödinger equation (including the coupling to the radiation field). Since the

127, 144102-1

high lying off-resonant part of the molecular spectrum should be incorporated, it is advisable to solve the Schrödinger equation by avoiding any state expansion. If this becomes possible with a sufficiently high precision, any type of light-induced transitions, as well as all the different NMT processes among them, can be accounted for. This direct nonperturbative approach has been demonstrated for atoms and diatomic molecules (with a fixed nuclear distance, see Refs. 20 and 21), as well as for one-dimensional model systems (avoiding the Born-Oppenheimer approximation).[22,23]

However, such a treatment cannot be applied to polyatomic systems. In these systems, because of computational difficulties, it is only possible to cover a restricted part of the overall electronic spectrum. A very reduced set of excited states φ_a, generalized to potential energy surfaces (PESs) for a selected set of nuclear coordinates, becomes available. A possible solution to this predicament is a description where all electronic states with energy levels far above the initial and final states of the NMT process are described in a way independent of the solution of the time-dependent Schrödinger equation.[1] For clarity we will call them nonresonant *secondary* states. Those states representing the initial and final states within the NMT process will then be named *primary* states. Since the secondary states enter the theory only via effective NMT coupling matrix elements **D**, there is no need to compute them directly. In this way, one may end up, for example, with an effective expression $\sim \mathbf{E}(t)\mathbf{D}\mathbf{E}(t)$ valid for nonresonant two-photon transitions and exclusively defined in the Hilbert space of primary states.

The use of effective coupling expressions to the radiation field is known from literature (see, e.g., Refs. 24 and 25) and the general approach of deriving such effective couplings is also known (see, for example, Refs. 1, 7, and 18), but it has been neither applied to the femtosecond spectroscopy nor used in the framework of optimal control theory (OCT). The latter represents an important theoretical tool for simulating an experiment using laser pulse control[26–28] (see also the recent formulation in Refs. 29–31).

In the following we shall show how NMT processes can be incorporated into a theory which only accounts for a very selected set of states (previously introduced here as the primary states). This enables us to establish an *effective* time-dependent Schrödinger equation with effective couplings to the radiation field including powers of the field strength and effective transition dipole operators. Such a treatment has two advantages. First, by solving a time dependent Schrödinger equation one avoids the computation of multiple time integrals necessary within perturbation theory. Second, and what is more important, a generalization of OCT to NMT processes becomes possible.

The present paper continues our earlier considerations of Ref. 19 and incorporates nonresonant three-photon transitions. It is organized as follows. After shortly describing the model and its specification to CpMn(CO)$_3$ (Refs. 10 and 18) in Sec. II, a systematic derivation of the effective coupling expressions will be given in Sec. III. Different approximations are introduced in Sec. IV, mainly based on a combination of the rotating wave approximation (RWA) and the slowly varying amplitude approximation (SVA). Afterwards,

Sec. V explains how to apply OCT if NMTs are involved. Corresponding applications to CpMn(CO)$_3$ can be found in Secs. IV and V. The paper ends with some concluding remarks.

II. THE MOLECULAR SYSTEM

The Hamiltonian of the polyatomic molecular system undergoing NMT processes is written as

$$H(t) = H_{\text{mol}} + H_{\text{field}}(t). \tag{2}$$

An expansion of the molecular part with respect to the adiabatic electronic states $|\varphi_\alpha\rangle$ gives

$$H_{\text{mol}} = \sum_\alpha H_\alpha(q)|\varphi_\alpha\rangle\langle\varphi_\alpha|. \tag{3}$$

The $H_\alpha(q)$ denote the related vibrational Hamiltonians (q abbreviates the set of vibrational coordinates). The eigenvalues and eigenfunctions of the vibrational Hamiltonian are written as $\hbar\varepsilon_{\alpha M} = \hbar\varepsilon_\alpha + \hbar\omega_{\alpha M}$ and $\chi_{\alpha M}$, respectively, where $\hbar\varepsilon_\alpha$ defines the electronic reference energy (minimum of the PES plus vibrational zero-point energy) and M denotes the set of vibrational quantum numbers. Accordingly, the adiabatic electronic-vibrational states $|\Psi_{\alpha M}\rangle = |\chi_{\alpha M}\rangle|\varphi_\alpha\rangle$ form a complete basis for the systems under consideration.

The part of Eq. (2) which describes the coupling to the radiation field is given in the standard dipole approximation and reads

$$H_{\text{field}}(t) = -\mathbf{E}(t)\hat{\boldsymbol{\mu}} \equiv -\mathbf{E}(t)\sum_{\alpha\neq\beta}\mathbf{d}_{\alpha\beta}|\varphi_\alpha\rangle\langle\varphi_\beta| + \text{H.c.}, \tag{4}$$

where $\hat{\boldsymbol{\mu}}$ is the molecular dipole operator, the $\mathbf{d}_{\alpha\beta}$ are its electronic matrix elements, and $\mathbf{E}(t)$ denotes the electric field strength. It will be written as

$$\mathbf{E}(t) = \tfrac{1}{2}\mathbf{n}E(t)e^{-i\omega t} + \text{c.c.}, \tag{5}$$

with $\mathbf{n}$ the unit vector of (linear) polarization, $E(t)$, the field envelope, and ω the carrier frequency.

In order to introduce the separation of the whole state space into the part of primary states and strongly off-resonant secondary states, we split up the φ_α into the set φ_x belonging to the state space of secondary states and a remaining set φ_a related to the primary state space. The latter may comprise the electronic ground state, $a=g$, and the first excited state with $a=e$ (some other excited states, $a=f,f',\ldots$, higher in energy may be included, too). It is advantageous to introduce the density of states (DOS) belonging to the secondary states,

$$\varrho(\Omega) = \sum_{x,K} \delta(\Omega - \varepsilon_{xK}). \tag{6}$$

If necessary, it can be reduced to a pure electronic DOS.

As indicated in the Introduction, numerical simulations will be presented for CpMn(CO)$_3$, for which *ab initio* potential energy surfaces and related properties are available.[10,32] Within the scope of this paper, we focus on nonresonant two-photon and three-photon transitions between the ground and the neutral electronic excited state c $^1A'$. The corresponding potential energy curves along the Mn–CO distance
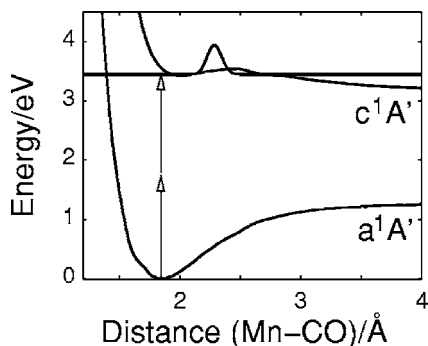
FIG. 1. *Ab initio* potential energy curves of CpMn(CO)$_3$ along the Mn–CO distance (adapted from Ref. 32). The arrows indicate a nonresonant two-photon transition from the electronic ground state $a\,^1A'$ to the electronic excited singlet state $c\,^1A'$. Also displayed is the vibrational target state $\chi_e^{(\mathrm{tar})}$ located in the excited electronic state which will be used later when applying the OCT.

with a schematic optical transition are illustrated in Fig. 1. At the employed level of theory (multireference configuration interaction based on complete active space self-consistent field calculations) the excited state $c\,^1A'$ is vertically reached at an excitation energy of 3.43 eV (or 362 nm). This state is bound until 2.442 Å, where a barrier appears due to avoided crossings with higher excited states.[32] Just before the Franck-Condon window (at 1.848 Å), the $c\,^1A'$ state also crosses the lower $b\,^1A'$ state. Because the nonadiabatic couplings between the $b\,^1A'$ and $c\,^1A'$ states are very weak,[32,33] they will be neglected in the forthcoming simulations.

III. EFFECTIVE SCHRÖDINGER EQUATION FOR NMT PROCESSES

In what follows we shortly recall the systematic way to derive an effective NMT Hamiltonian as described in Ref. 19. The effective Hamiltonian will enter into an effective Schrödinger equation exclusively defined in the space of primary states. The approach uses standard projection operator techniques and is based on the projector into the space of primary states,

$$\hat{P} = \sum_a |\varphi_a\rangle\langle\varphi_a|. \tag{7}$$

Its orthogonal complement is denoted by

$$1 - \hat{P} \equiv \hat{Q} = \sum_x |\varphi_x\rangle\langle\varphi_x|. \tag{8}$$

By introducing $\hat{P}$ and $\hat{Q}$ we obtain the primary and secondary states as $|\Psi_1(t)\rangle = \hat{P}|\Psi(t)\rangle$ and as $|\Psi_2(t)\rangle = \hat{Q}|\Psi(t)\rangle$, respectively, where $\Psi(t)$ is an arbitrary state defined in the complete Hilbert space.

Standard projection operator techniques yield a closed equation for the primary states (see Ref. 19):

$$i\hbar\frac{\partial}{\partial t}|\Psi_1(t)\rangle = H_1(t)|\Psi_1(t)\rangle + \int_{t_0}^{t} d\bar{t}\,K_{\mathrm{field}}(t,\bar{t})|\Psi_1(\bar{t})\rangle, \tag{9}$$

with $H_1(t) = H_{\mathrm{mol}}^{(1)} + H_{\mathrm{field}}^{(1)}(t) = \hat{P}H(t)\hat{P}$ and with the time-integral kernel

$$K_{\mathrm{field}}(t,\bar{t}) = -\frac{i}{\hbar}\hat{P}H_{\mathrm{field}}(t)\hat{Q}U_2^{(\mathrm{mol})}(t-\bar{t})$$

$$\times S_2(t,\bar{t};\mathbf{E})\hat{Q}H_{\mathrm{field}}(\bar{t})\hat{P}. \tag{10}$$

The originally appearing time-evolution operator $U_2(t,\bar{t};\mathbf{E})$ defined by $H_2(t) = H_{\mathrm{mol}}^{(2)} + H_{\mathrm{field}}^{(2)}(t) = \hat{Q}H(t)\hat{Q}$ has been separated into $U_2^{(\mathrm{mol})}(t-\bar{t})$ and into $S_2(t,\bar{t};\mathbf{E})$. The S operator is defined in the standard way by $H_{\mathrm{field}}^{(2)}(t)$ taken in the interaction representation given by $U_2^{(\mathrm{mol})}$. The obtained time-integral kernel accounts for all NMT processes realized by the coupling to the manifold of off-resonant states. Since the latter have been projected out, the resulting reduced time-dependent Schrödinger equation is time nonlocal, showing a memory effect.

Since Eq. (9) has been derived without any approximation, its solution $\Psi_1(t)$ should be identical with $\Psi(t)$ projected into the space of primary states. If a particular approximation for K_{field} is taken, however, the quality of the result has to be judged by separate computations. Such a problem arises since the kernel K_{field}, Eq. (10), already includes a complete summation with respect to $\mathbf{E}$. It is covered via S_2 which has to be approximated when carrying out concrete computations. Once such an approximation has been introduced one has to check separately if Ψ_1 obtained by a direct solution of Eq. (9) describes the main features of the dynamics. We will proceed in this manner in the following. First, we set

$$K_{\mathrm{field}}(t,\bar{t}) = K_{\mathrm{field}}^{(2)}(t,\bar{t}) + K_{\mathrm{field}}^{(3)}(t,\bar{t}) + \cdots, \tag{11}$$

where $K_{\mathrm{field}}^{(2)}$ and $K_{\mathrm{field}}^{(3)}$ are of second and third powers in the field strength, respectively. They are obtained in replacing $S_2(t,\bar{t};\mathbf{E})$ in Eq. (10) by an expansion up to a linear contribution with respect to the field strength. In a second step, we have to check the validity of the K_{field} expansion. Before doing this it is useful to introduce primary system electronic matrix elements of the two types of time-integral kernels. We obtain

$$K_{ab}^{(2)}(t,\bar{t}) = -\mathbf{D}_{ab}^{(2)}(t-\bar{t})\mathbf{E}(t)\mathbf{E}(\bar{t}) \tag{12}$$

and

$$K_{ab}^{(3)}(t,\bar{t}) = -\int_{\bar{t}}^{t} dt_1 \mathbf{D}_{ab}^{(3)}(t,t_1,\bar{t})\mathbf{E}(t)\mathbf{E}(t_1)\mathbf{E}(\bar{t}). \tag{13}$$

The effective coupling matrix elements entering $K_{ab}^{(2)}$ read

$$\mathbf{D}_{ab}^{(2)}(t-\bar{t}) = \frac{i}{\hbar}\langle\varphi_a|\hat{\boldsymbol{\mu}}\hat{Q}U_2^{(\mathrm{mol})}(t-\bar{t})\hat{Q}\hat{\boldsymbol{\mu}}|\varphi_b\rangle$$

$$= \frac{i}{\hbar}\sum_x \mathbf{d}_{ax}e^{-iH_x(t-\bar{t})/\hbar}\mathbf{d}_{xb}. \tag{14}$$

The second expression is obtained by introducing an expansion with respect to secondary electronic states. In the same manner we get the coupling matrix elements appearing in $K_{ab}^{(3)}$:

$$\mathbf{D}_{ab}^{(3)}(t-t_1, t_1-\overline{t}) = \frac{1}{\hbar^2} \langle \varphi_a | \hat{\boldsymbol{\mu}} \hat{Q} U_2^{(\text{mol})}(t-t_1)$$

$$\times \hat{Q} \hat{\boldsymbol{\mu}} \hat{Q} U_2^{(\text{mol})}(t_1-\overline{t}) \hat{Q} \hat{\boldsymbol{\mu}} | \varphi_b \rangle$$

$$= \frac{1}{\hbar^2} \sum_{x,y} \mathbf{d}_{ax} e^{-iH_x(t-t_1)/\hbar} \mathbf{d}_{xy} e^{-iH_y(t_1-\overline{t})/\hbar} \mathbf{d}_{yb}. \tag{15}$$

If the time-dependent Schrödinger equation [Eq. (9)] is expanded with respect to the primary electronic states, we will get the following coupled equations of motion for the vibrational wave functions $\chi_a(t) = \langle \varphi_a | \Psi_1(t) \rangle$:

$$i\hbar \frac{\partial}{\partial t} \chi_a(t) = H_a \chi_a(t) - \mathbf{E}(t) \sum_b \mathbf{d}_{ab} \chi_b(t)$$

$$- \sum_b \int_{t_0}^{t} d\overline{t} \mathbf{D}_{ab}^{(2)}(t-\overline{t}) \mathbf{E}(t) \mathbf{E}(\overline{t}) \chi_b(\overline{t})$$

$$- \sum_b \int_{t_0}^{t} d\overline{t} \int_{\overline{t}}^{t} dt_1 \mathbf{D}_{ab}^{(3)}(t-t_1, t_1-\overline{t})$$

$$\times \mathbf{E}(t) \mathbf{E}(t_1) \mathbf{E}(\overline{t}) \chi_b(\overline{t}). \tag{16}$$

Besides single-photon transitions described by the second term on the right-hand side, the equations account for two- and three-photon nonresonant transitions. As already stated, however, there is not any distinct criteria telling us up to which field strengths $\mathbf{E}$ the wave function computed with $K_{\text{field}}^{(2)}$ and $K_{\text{field}}^{(3)}$ is correct. Here, we restrict to those $\mathbf{E}$ which induce a fourth-order or sixth-order dependence of the excited-state population on $\mathbf{E}$. This is the limit of perturbation theory and should be correct, but it has the advantage of being generated via a complete solution of the time-dependent Schrödinger equation. The time nonlocality, however, represents a technical disadvantage which should be overcome by approximations explained in the subsequent section.

IV. NMT PROCESSES DESCRIBED IN THE COMBINED RWA AND SVA

Next, the RWA will be combined with the SVA in order to introduce an approximation scheme leading to time-local Schrödinger equations. First, to arrive at the RWA we expand the primary state vibrational wave functions with respect to powers of the basic oscillation $\sim \exp(-i\omega t)$ of the applied pulse and obtain

$$\chi_a(t) = \sum_n e^{-in\omega t} \chi_a(n;t), \tag{17}$$

with n running over all integers. This expansion changes the coupled time-dependent Schrödinger equations [Eq. (16)] to

$$\sum_n e^{-in\omega t} \left(\left[i\hbar \frac{\partial}{\partial t} + n\hbar\omega - H_a \right] \chi_a(n;t) \right.$$

$$+ \frac{1}{2} \sum_b d_{ab} [E(t) \chi_b(n-1;t) + E^*(t) \chi_b(n+1;t)]$$

$$\left. - \sum_b \int_{t_0}^{t} d\overline{t} K_{ab}(t,\overline{t}) e^{in\omega(t-\overline{t})} \chi_b(n;t) \right) = 0. \tag{18}$$

Note the introduction of $d_{ab} = \mathbf{n} d_{ab}$ and the abbreviation of $K_{ab}^{(2)} + K_{ab}^{(3)}$ by K_{ab}. These latter quantities also depend on the field amplitudes $E(t)$ and $E^*(t)$. In order to get the RWA, one assumes that the time dependence of the expression in the large bracket of Eq. (18) is slow compared to the oscillations with multiples of ω. It results to

$$i\hbar \frac{\partial}{\partial t} \chi_a(n;t) = [n\hbar\omega - H_a] \chi_a(n;t)$$

$$- \frac{1}{2} \sum_b d_{ab} [E(t) \chi_b(n-1;t)$$

$$+ E^*(t) \chi_b(n+1;t)]$$

$$+ \sum_b \int_{t_0}^{t} d\overline{t} K_{ab}(t,\overline{t}) e^{in\omega(t-\overline{t})} \chi_b(n;\overline{t}). \tag{19}$$

The required slow time dependence is guaranteed if a restriction to those n is taken which makes the energetic difference corresponding to $n\hbar\omega - H_a$ much smaller than $\hbar\omega$. Once Eq. (19) has been solved, the electronic level populations follow as

$$P_a(t) = \sum_n \langle \chi_a(n;t) | \chi_a(n;t) \rangle. \tag{20}$$

Note that this expression neglects small contributions being off-diagonal with respect to the index n and oscillating with multiples of ω.

In the following we present results for the primary system restricted to an electronic two-level system with the electronic ground state φ_g and the first excited state φ_e. To have reference cases for the novel three-photon transition, we shortly recall single- and two-photon transitions (see also Ref. 19). To get the RWA description of single-photon transitions, we concentrate on the second term of the right-hand side of Eq. (19). Moreover, the multitude of functions $\chi_a(n;t)$ determining the complete vibrational wave functions $\chi_a(t)$ is restricted to $\chi_g(0;t)$ and $\chi_e(1;t)$. This leads to

$$i\hbar \frac{\partial}{\partial t} \chi_g(0;t) = H_g \chi_g(0;t) - \frac{1}{2} d_{ge} E^*(t) \chi_e(1;t) \tag{21}$$

and

$$i\hbar \frac{\partial}{\partial t} \chi_e(1;t) = (H_e - \hbar\omega) \chi_e(1;t) - \frac{1}{2} d_{eg} E(t) \chi_g(0;t). \tag{22}$$

The two equations of motion are equivalent to a RWA Hamiltonian $H^{(\text{RWA})}(t) = H_{\text{mol}}^{(\text{RWA})} + H_{\text{field}}^{(\text{RWA})}(t)$. The expression for $H_{\text{mol}}^{(\text{RWA})}$ is identical to the two-level version of $H_{\text{mol}}^{(1)}$ (except that H_e has to be replaced by $H_e - \hbar\omega$), and the molecule field coupling Hamiltonian takes the well-known form $H_{\text{field}}^{(\text{RWA})}(t) = -(1/2)E(t) d_{eg} | \varphi_e \rangle \langle \varphi_g | - (1/2)E^*(t) d_{ge} | \varphi_g \rangle \langle \varphi_e |$. This is just

the quantity we will utilize later when formulating the OCT in the framework of the RWA.

Two-photon transitions are included in the time nonlocal K_{field} term of Eq. (19) [by the $K_{field}^{(2)}$ contribution to K_{field}]. A restriction to expansion functions $\chi_a(n;t)$ which slowly vary in time is achieved by considering $\chi_g(0;t)$ and $\chi_e(2;t)$ only. Moreover, it has been assumed that the field amplitude $E(t)$ and the expansion functions $\chi_g(0;t)$ and $\chi_e(2;t)$ display such a weak time dependence that they can be taken out of the time integral. The Appendix explains this procedure in some detail. It leads to (see also Ref. 19)

$$i\hbar\frac{\partial}{\partial t}\chi_g(0;t) = H_g\chi_g(0;t) - \tfrac{1}{2}d_{gg}^{(2)}|E(t)|^2\chi_g(0;t)$$
$$- \tfrac{1}{4}d_{ge}^{(2)}E^{*2}(t)\chi_e(2;t) \tag{23}$$

and

$$i\hbar\frac{\partial}{\partial t}\chi_e(2;t) = (H_e - 2\hbar\omega)\chi_e(2;t) - \tfrac{1}{2}d_{ee}^{(2)}|E(t)|^2\chi_e(2;t)$$
$$- \tfrac{1}{4}d_{eg}^{(2)}E^2(t)\chi_g(0;t). \tag{24}$$

Here, the RWA version of the effective molecule field coupling Hamiltonian reads

$$H_{field}^{(RWA)}(t) = -\tfrac{1}{2}\sum_{a=g,e}|E(t)|^2 d_{aa}^{(2)}|\varphi_a\rangle\langle\varphi_a| - \tfrac{1}{4}E^2(t)d_{eg}^{(2)}|\varphi_e\rangle$$
$$\times\langle\varphi_g| - \tfrac{1}{4}E^{*2}(t)d_{ge}^{(2)}|\varphi_g\rangle\langle\varphi_e|. \tag{25}$$

Besides two-photon transitions, the Hamiltonian also contains polarizability terms $\sim d_{gg}^{(2)}$ and $\sim d_{ee}^{(2)}$, which introduce an ac Stark shift of both levels involved.

Three-photon transitions can be handled in the same way as demonstrated for two-photon transitions. They are accounted for by the $K_{field}^{(3)}$ contribution to the nonlocal K_{field} term of Eq. (19). The RWA results in a restriction to $\chi_g(0;t)$ and $\chi_e(3;t)$. If combined with the SVA, we arrive at (for details see the Appendix)

$$i\hbar\frac{\partial}{\partial t}\chi_g(0;t) = H_g\chi_g(0;t) - \tfrac{1}{8}d_{ge}^{(3)}E^{*3}(t)\chi_e(3;t) \tag{26}$$

and

$$i\hbar\frac{\partial}{\partial t}\chi_e(3;t) = (H_e - 3\hbar\omega)\chi_e(3;t) - \tfrac{1}{8}d_{eg}^{(3)}E^3(t)\chi_g(0;t). \tag{27}$$

The RWA version of the related coupling Hamiltonian to the radiation field reads

$$H_{field}^{(RWA)}(t) = -\tfrac{1}{8}E^3(t)d_{eg}^{(3)}|\varphi_e\rangle\langle\varphi_g| - \tfrac{1}{8}E^{*3}(t)d_{ge}^{(3)}|\varphi_g\rangle\langle\varphi_e|. \tag{28}$$

In contrast to the two-photon transition coupling, it does not contain ground- and excited-state polarizabilities.

Results for the excited-state population $P_e(t)$ referring to $CpMn(CO)_3$ and a 100 fs pulse with different field strengths are shown in Fig. 2 for nonresonant two-photon transitions and in Fig. 3 for nonresonant three-photon transitions. To get the two-photon coupling matrix elements $d_{ab}^{(2)}$, we take the
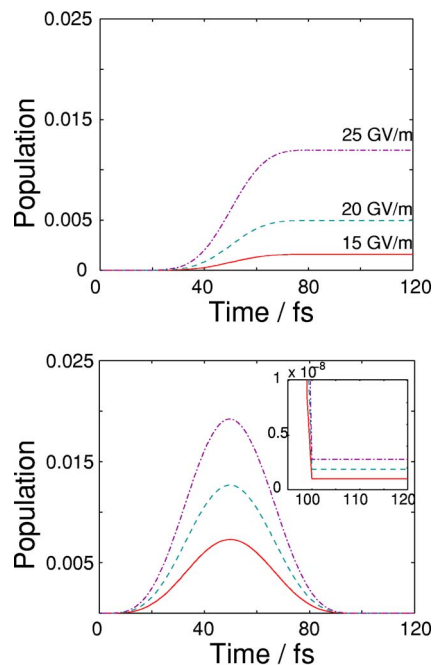
FIG. 2. Nonresonant two-photon transitions in $CpMn(CO)_3$ (upper panel) compared with nonresonant single-photon transitions (lower panel). Shown are the temporal evolutions of the excited-state population $P_e(t)$ [of the $c\ ^1A'$ state, see also Eq. (20)]. Excitation has been achieved by a pulse with photon energy $\hbar\omega = 1.715$ eV, envelope $\sin^2(\pi t/\tau)$, and duration of $\tau = 100$ fs. The effective two-photon coupling is characterized by $d_{eff} = 1$ D and $\bar{\varrho} = 50$/eV and the single-photon transition by $d_{eg} = 1$ D. The maximum field strength has been varied as indicated. The insert enlarges the population which has been achieved by single-photon excitation at the end of the pulse.

approximation $\bar{\varrho}d_{eff}^2/\hbar$, Eq. (A5). The approximation relates the two-photon coupling matrix elements to the mean DOS $\bar{\varrho}$ of the secondary states and to the square of an effective (mean) transition dipole moment d_{eff} between primary and secondary states. The three-photon coupling matrix elements $d_{ab}^{(3)}$ have been estimated according to $\bar{\varrho}^2 d_{eff}^3/\hbar^2$, Eq. (A12). Moreover, one can easily prove that the excited-state populations presented in Fig. 2 are proportional to the fourth power of the field strength and those of Fig. 3 to the sixth power. This behavior indicates that we are just in the range of perturbation theory for nonresonant two-photon transitions as well as for nonresonant three-photon transitions, i.e., the results are consistent with the expansion in Eq. (11).

For comparison, the population achieved by a strongly off-resonant single-photon transition is also shown. It only results in an intermediate population during the pulse action with a residual value after excitation of about four to five orders of magnitude smaller than the respective NMT value (see inserts of Figs. 2 and 3).

V. OCT OF NMT PROCESSES

In the following, the presented version of nonresonant two-photon and three-photon transitions shall be embedded into the OCT. The standard version of OCT (see, e.g., Refs. 11–13) assumes that a molecular state, the target state Ψ_{tar}, is attainable by a laser-driven molecular wave function $\Psi(t)$ at time t_f, or in other words, that the overlap expression $|\langle\Psi_{tar}|\Psi(t_f)\rangle|^2$ be unity. To determine the laser pulse which
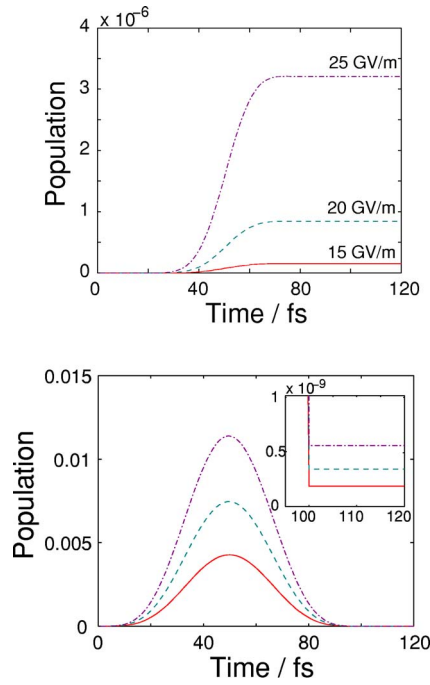
FIG. 3. Nonresonant three-photon transition in CpMn(CO)$_3$ (upper panel) compared with a nonresonant single-photon transition (lower panel). Shown are the temporal evolutions of the excited-state population $P_e(t)$ [of $c\,^1A'$ state, see also Eq. (20)]. Excitation has been achieved by a pulse with photon energy $\hbar\omega = 1.143$ eV, envelope $\sin^2(\pi t/\tau)$, and duration of $\tau = 100$ fs. The effective three-photon coupling is characterized by $d_{\mathrm{eff}} = 1$ D and $\bar{\varrho} = 50/\mathrm{eV}$ and the single-photon transition by $d_{eg} = 1$ D. The maximum field strength has been varied as indicated. The insert enlarges the population which has been achieved by single-photon excitation at the end of the pulse.

drives the system to its predefined target state (the *optimal pulse*) one considers the overlap $|\langle\Psi_{\mathrm{tar}}|\Psi(t_f)\rangle|^2$ to be a functional of the field strength $\mathbf{E}(t)$. An extremum of this functional should be obtained if the optimal pulse is known. To this end, OCT is formulated as a task which solves for an extremum with the constraint that the field strength is of a finite value. In a more general formulation, one introduces the observable

$$\mathcal{O}[\mathbf{E}] = \langle\Psi(t_f)|\hat{O}|\Psi(t_f)\rangle \tag{29}$$

to be optimized in the particular control task. Its optimized value is known as the *control yield* (setting $\hat{O} = |\Psi_{\mathrm{tar}}\rangle\langle\Psi_{\mathrm{tar}}|$ we move back to the initially introduced standard version of OCT).

To apply OCT with the incorporation of the RWA, we introduce the control functional as

$$J[E,E^*] = \mathcal{O}[E,E^*] - \lambda \int_{t_0}^{t_f} dt\,|E(t)|^2. \tag{30}$$

If defined in the appropriate way, the observable $\mathcal{O}$ and the control functional J appear as quantities depending only on the field envelope $E(t)$ (as well as on its conjugate complex counterpart); thus, any oscillation with the carrier frequency ω and multiples of it are absent. The solution of the OCT results in an optimal envelope $E(t)$ which leads to the optimal pulse only after inserting $E(t)$ into Eq. (5). Nevertheless, the approach to optimize the envelope is as flexible as the

original OCT since, for example, any modulation of the carrier frequency can be accounted for by a proper change of $E(t)$.

To determine the extremum of $J[E,E^*]$ and to derive a relation fixing the optimal pulse, we take the functional derivative of $J[E,E^*]$, Eq. (30), with respect to $E^*(t)$. Afterwards, the result has to be set equal to zero and we arrive at (see Ref. 19 for details)

$$\begin{aligned}
E(t) = &-\frac{i}{\hbar\lambda}\Bigg(\langle\Psi(t_f)|\hat{O}U(t_f,t)\frac{\partial H_{\mathrm{field}}^{(\mathrm{RWA})}(t)}{\partial E^*(t)}|\Psi(t)\rangle \\
&-\left[U(t_f,t)\frac{\partial H_{\mathrm{field}}^{(\mathrm{RWA})}(t)}{\partial E(t)}|\Psi(t)\rangle\right]^*\hat{O}|\Psi(t_f)\rangle\Bigg) \\
= &-\frac{i}{\hbar\lambda}\Bigg(\langle\Theta(t)|\frac{\partial H_{\mathrm{field}}^{(\mathrm{RWA})}(t)}{\partial E^*(t)}|\Psi(t)\rangle \\
&-\left[\frac{\partial H_{\mathrm{field}}^{(\mathrm{RWA})}(t)}{\partial E(t)}|\Psi(t)\rangle\right]^*|\Theta(t)\rangle\Bigg). \tag{31}
\end{aligned}$$

Here, $\partial H_{\mathrm{field}}^{(\mathrm{RWA})}(t)/\partial E^*(t)$ denotes the ordinary derivative of the RWA field coupling Hamiltonian with respect to the field envelope. Note also the inserted abbreviation

$$|\Theta(t)\rangle = U(t,t_f)\hat{O}|\Psi(t_f)\rangle \equiv \sum_a |\vartheta_a(t)\rangle|\varphi_a\rangle, \tag{32}$$

which indicates propagation backwards in time from the "initial" value

$$\hat{O}|\Psi(t_f)\rangle = \langle\Psi_{\mathrm{tar}}|\Psi(t_f)\rangle|\Psi_{\mathrm{tar}}\rangle = \langle\Psi_{\mathrm{tar}}|\Psi(t_f)\rangle\sum_a |\chi_a^{(\mathrm{tar})}\rangle|\varphi_a\rangle \tag{33}$$

at time t_f to the actual value at time t.

Equation (31) can be considered as a self-consistency relation for the optimal field. Its concrete form depends on the specific type of RWA field coupling Hamiltonian. In the subsequent section we present such self-consistency relation for nonresonant two- and three-photon transitions. Moreover, we simply identify $\hat{O}$ with the projection onto the vibrational state $\chi_e^{(\mathrm{tar})}$ positioned in the excited electronic state (see Fig. 1), i.e. we set

$$\begin{aligned}
\mathcal{Q}[E,E^*] &= \langle\Psi(t_f)| \times |\chi_e^{(\mathrm{tar})}\varphi_e\rangle\langle\varphi_e\chi_e^{(\mathrm{tar})}| \times |\Psi(t_f)\rangle \\
&\equiv |\langle\chi_e(t_f)|\chi_e^{(\mathrm{tar})}\rangle|^2. \tag{34}
\end{aligned}$$

To have a reference case at hand, we start with the presentation of this relation for the standard case of single-photon transitions.

A. The reference case: OCT for single-photon transitions

When considering single-photon transitions, the general form of the self-consistency relation is standard (see, for example, Ref. 13). Formulating it in the framework of the RWA, however, found less attention. It reads as
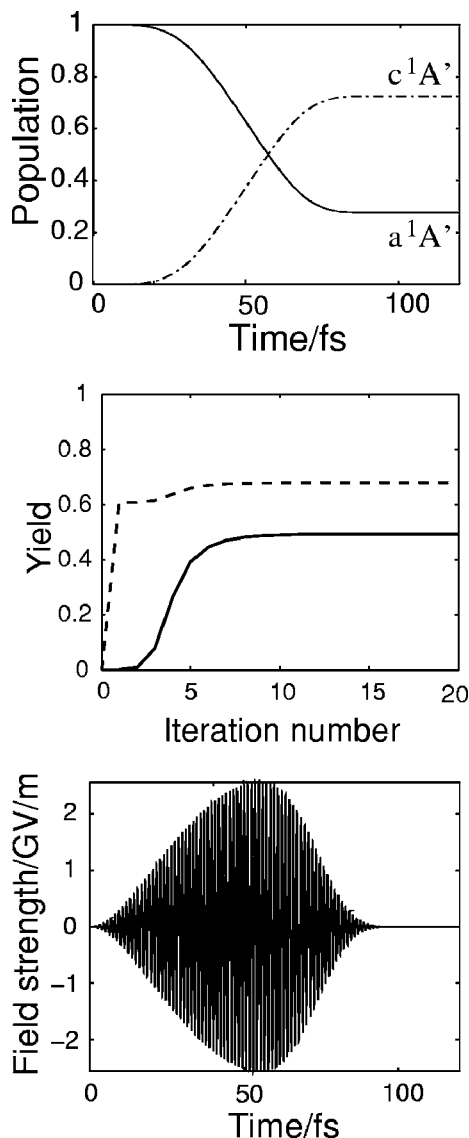
FIG. 4. Laser pulse control in CpMn(CO)$_3$ based on a single-photon transition into the excited $c\ ^1A'$ electronic state [target vibrational wave packet is positioned according to Fig. 1, see also Eq. (34)]. The photon energy referring to the carrier wave amounts to 3.43 eV and the final time of the control task equals 100 fs (the field amplitude of the pulse which initiates the iterative solution of the OCT is 10 GV/m and d_{eg}=1 D). Upper panel: total population of the ground state (full line) and of the excited state (dashed-dotted line); middle panel: control yield (full line) and renormalized control yield (dashed line); lower panel: temporal evolution of the optimal pulse.

$$E(t) = \frac{id_{eg}}{2\hbar\lambda}(\langle\vartheta_g(t)|\chi_e(t)\rangle - \langle\chi_g(t)|\vartheta_e(t)\rangle). \tag{35}$$

Following Refs. 29–31 this expression is inserted into the equations for forward propagation (vibrational wave functions χ_a) and backward propagation (vibrational wave functions ϑ_a). Then, the resulting coupled nonlinear Schrödinger equations are solved iteratively.

The target is set to displace the wave packet in the $c\ ^1A'$ state to the turning point located at 2.23 Å, as shown in Fig. 1. Figure 4 displays some quantities obtained from the solution of this control task. The temporal behavior of the electronic level populations indicates a rather strong excitation

with an about 60% population of the excited state. The related control yield (already reached after less than ten iterations) lies at about 0.5.

If laser pulse control is considered with the target in an excited electronic state, the introduction of the renormalized control yield

$$q[E,E^*] = \frac{\mathcal{Q}[E,E^*]}{P_e(t_f)} \tag{36}$$

is rather useful. It relates the extent to reach the target state to the overall excited-state population. In the present case q arrives at a value clearly above $\mathcal{Q}$. The optimal field also shown in Fig. 4 is directly deduced from Eq. (5) as $\mathbf{n}E(t)$ = Re[$E(t)$exp($i\omega t$)] by inserting the complex valued optimal field envelope. It shows a pronounced asymmetry.

B. OCT for nonresonant two-photon transitions

The optimal field self-consistency relation has been derived in Ref. 19 and reads

$$E(t) = \frac{i}{2\hbar\lambda}\Bigg(\sum_{a=g,e} d_{aa}^{(2)}\langle\vartheta_a(t)|\chi_a(t)\rangle E(t) + d_{ge}^{(2)}$$
$$\times\langle\vartheta_g(t)|\chi_e(t)\rangle E^*(t) - \sum_{a=g,e} d_{aa}^{(2)}\langle\chi_a(t)|\vartheta_a(t)\rangle E(t)$$
$$- d_{ge}^{(2)}\langle\chi_g(t)|\vartheta_e(t)\rangle E^*(t)\Bigg). \tag{37}$$

The time-dependent Schrödinger equations for the vibrational wave functions are given by Eqs. (23) and (24) as well as by the respective versions for the backward propagation. The explicit appearance of the field envelope on the right-hand site makes this self-consistency relation for the optimal field different from the standard single-photon version [see Eq. (35)]. This requires a modification of the scheme to determine the optimal field, a work postponed to the future.

Here, the procedure to compute the optimal field is put into a somewhat approximate but very efficient form. First, we neglect the terms proportional to $d_{aa}^{(2)}$ since they only result in minor corrections. Then, two-photon transitions can be completely characterized by the effective field envelope

$$\mathcal{E}(t) = E^2(t). \tag{38}$$

We replace $\int_{t_0}^{t_f}dt|E(t)|^2$ in Eq. (30) by the expression $\int_{t_0}^{t_f}dt|E(t)|^4/2$ and afterwards express the optimal field self-consistency relation by $\mathcal{E}$. This yields

$$\mathcal{E}(t) = \frac{id_{ge}^{(2)}}{2\hbar\lambda}(\langle\vartheta_g(t)|\chi_e(t)\rangle + \langle\chi_g(t)|\vartheta_e(t)\rangle). \tag{39}$$

The introduction of $\mathcal{E}$ is also possible in the related time-dependent Schrödinger equations in Eqs. (23) and (24). Hence, the determination of the optimal field can be done in the standard way, but now focusing on $\mathcal{E}(t)$.

Figure 5 shows the same quantities as Fig. 4, however, following from the solution of the OCT based on two-photon transitions. The behavior of the electronic level populations, of the control yield, and the renormalized control yield are similar to those in the case of single-photon transitions, Fig.
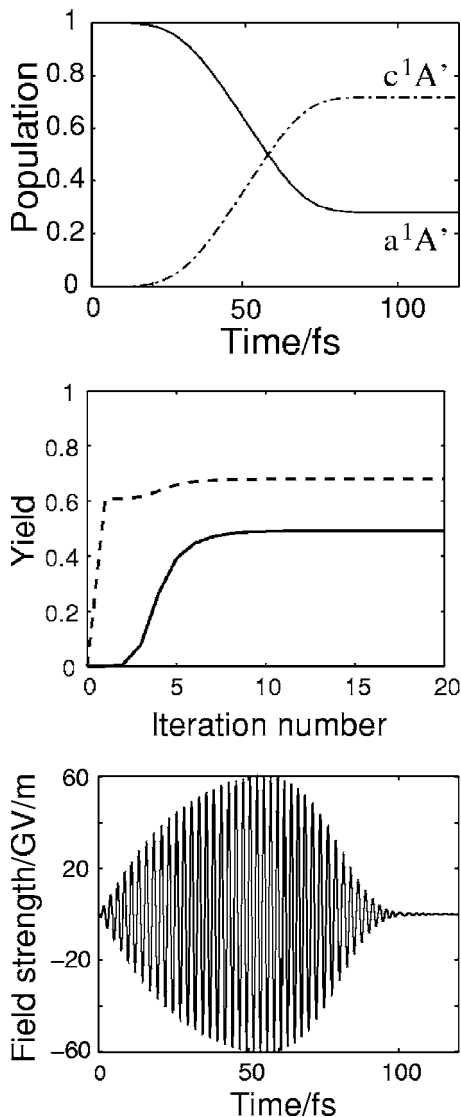
FIG. 5. Laser pulse control in CpMn(CO)$_3$ based on a nonresonant two-photon transition into the excited $c\ ^1A'$ electronic state [target vibrational wave packet is positioned according to Fig. 1, see also Eq. (34)]. The photon energy referring to the carrier wave amounts to 1.75 eV and the final time of the control task equals 100 fs (the field amplitude of the pulse which initiates the iterative solution of the OCT is 10 GV/m). The effective two-photon coupling is characterized by $d_{eff}=1$ D and $\bar{\varrho}=50/$eV. Upper panel: total population of the ground state (full line) and of the excited state (dashed-dotted line); middle panel: control yield (full line) and renormalized control yield (dashed line); lower panel: temporal evolution of the optimal pulse.

4. The obtained optimal field pulse $\mathbf{n}E(t)$, however, deduced from $\mathcal{E}(t)$, is more intense and with a slightly different shape.

C. OCT with nonresonant three-photon transitions

OCT based on three-photon transitions is formulated similar to the case of two-photon transitions in the foregoing section. First, we note

$$\frac{\partial H_{\text{field}}^{(\text{RWA})}(t)}{\partial E^*(t)} = -\frac{3}{8}E^{*2}(t)d_{ge}^{(3)}|\varphi_g\rangle\langle\varphi_e| = \left(\frac{\partial H_{\text{field}}^{(\text{RWA})}(t)}{\partial E(t)}\right)^*,$$

(40)

which yields

$$E(t) = \frac{3id_{ge}^{(3)}}{8\hbar\lambda}(\langle\vartheta_g(t)|\chi_e(t)\rangle + \langle\chi_g(t)|\vartheta_e(t)\rangle)E^{*2}(t).$$ (41)

The time-dependent Schrödinger equations for the vibrational wave functions are given by Eqs. (26) and (27) as well as the respective versions for the backward propagation.

Again, the procedure to compute the optimal field can be put into a more efficient form by introducing

$$\mathcal{E}(t) = E^3(t)$$ (42)

for the three-photon transition. Since the coupling terms to the radiation field are absent which are diagonal with respect to the electronic quantum numbers [polarizability terms proportional to $d_{aa}^{(2)}$ in Eq. (25)], the effective field $\mathcal{E}$ could be introduced from the beginning. However, we directly rewrite Eq. (41) replacing $\int_{t_0}^{t_f}dt|E(t)|^2$ in Eq. (30) by $\int_{t_0}^{t_f}dt|E(t)|^6/3$. Then, the functional derivative with respect to $E^*(t)$ leads on the right-hand side of Eq. (41) to $E^{*2}(t)E^3(t)$ instead of $E(t)$. We arrive at

$$\mathcal{E}(t) = \frac{3id_{ge}^{(3)}}{8\hbar\lambda}(\langle\vartheta_g(t)|\chi_e(t)\rangle + \langle\chi_g(t)|\vartheta_e(t)\rangle).$$ (43)

Such a replacement is also possible in the related time-dependent Schrödinger equations in Eqs. (26) and (27) and the determination of the optimal field can be done in the standard way but primarily focusing on $\mathcal{E}(t)$.

The solution of the control task (target state according to Fig. 1) is displayed in Fig. 6. The electronic level populations, as well as the reduced control yield, behave similar to the single-photon and two-photon cases (see Figs. 4 and 5, respectively). The overall control yield $\mathcal{Q}$, however, needs some further iteration to be built up, and the optimal pulse has a stronger field strength (it also appears broader as the ones calculated earlier).

The field strength used here as well as in the preceding section to control two-photon transitions is already in the so-called strong-field regime and may induce an additional process accompanying the described two- or three-photon transitions from the ground to the first excited state. Therefore, the results have to be understood as a reference for demonstration. However, it has been already discussed in our preliminary description of two-photon transitions in Ref. 19 that a decrease of the field strength into a reasonable range is easily possible, yet maintaining the renormalized control yield q. Of course the control yield $\mathcal{Q}$ is reduced drastically. We disclaim to present respective curves but state that the already computed values of the renormalized control yield can be reproduced by field strengths two or three orders of magnitude smaller than those presented beforehand.

VI. CONCLUSIONS

Nonresonant multiphoton transitions have been described for polyatomic systems. Since a complete solution of the time-dependent Schrödinger equation accounting for all electronic levels is impossible, a description in the framework of an effective Schrödinger equation has been given. It only accounts for all those levels which are directly incorpo-
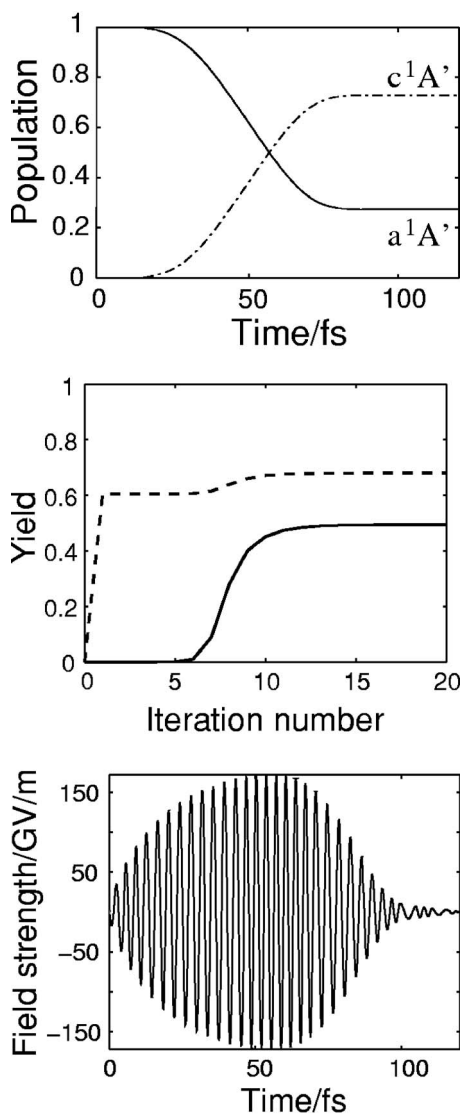
FIG. 6. Laser pulse control in CpMn(CO)$_3$ based on a nonresonant three-photon transition into the excited $c\,^1A'$ electronic state [target vibrational wave packet is positioned according to Fig. 1, see also Eq. (34)]. The photon energy referring to the carrier wave amounts to 1.143 eV and the final time of the control task equals 100 fs (the field amplitude of the pulse which initiates the iterative solution of the OCT is 10 GV/m). The effective three-photon coupling is characterized by $d_{eff}=1$ D and $\bar{\varrho}=50/\text{eV}$. Upper panel: total population of the ground state (full line) and of the excited state (dashed-dotted line); middle panel: control yield (full line) and renormalized control yield (dashed line); lower panel: temporal evolution of the optimal pulse.

rated in the optical transitions as initial, intermediate, and final states. The multitude of off-resonant states are considered via effective coupling matrix elements.

While this type of Schrödinger equation is nonlocal in time, the rotating wave approximation has been combined with a slowly varying amplitude approximation to arrive at time-local equations. The latter approximation became possible since the laser pulse field strength, as well as the molecular vibrational wave functions, has been expanded with respect to multiples of the laser pulse carrier wave (oscillating with a photon energy in the optical range).

The presented approach has been implemented to nonresonant two-photon and three-photon transitions taking

place between the electronic ground state and the first excited state of CpMn(CO)$_3$. Moreover, the optimal control theory has been adopted to these nonresonant two-photon and three-photon transitions.

Combining two-photon and three-photon transitions, for example, to reach a higher ionic state in an electronic three-level system is straightforward in the presented general approach. Simulations of the complete two-photon and three-photon excitations and ionization pump-probe process in CpMn(CO)$_3$ as it has been already discussed in the experiment[10] are in progress.

ACKNOWLEDGMENT

APPENDIX: THE MOLECULE FIELD COUPLING, THE RWA, AND THE SVA

Based on the expansion [Eq. (17)] of the vibrational wave functions and the total time-dependent Schrödinger equation, we detail in the following how to achieve a simplification of the time-nonlocal terms in Eq. (16) by applying the RWA and the SVA. Respective calculations for the two-photon term have been already presented in Ref. 19 and are shortly quoted here only for completeness.

Let us consider the time-nonlocal term of Eq. (16) to be proportional to $\mathbf{D}_{ab}^{(2)}$. We note Eq. (5) for the field strength, the expansion according to Eq. (17), and the abbreviation $D_{ab}^{(2)}=\mathbf{n}\mathbf{D}_{ab}^{(2)}\mathbf{n}$. Moreover, we introduce products of factors oscillating with $\exp(-in\omega t)$ as well as with $\exp(in\omega t)$. All terms can be arranged in such a way that they have the common prefactor $\exp(-in\omega t)$. It requires to move in part from $\chi_b(n;\bar{t})$ to $\chi_b(n\pm2;\bar{t})$. The introduction of the difference time $\tau=t-\bar{t}$ results in

$$-\sum_b \int_{t_0}^t d\bar{t}\,\mathbf{D}_{ab}^{(2)}(t-\bar{t})\mathbf{E}(t)\mathbf{E}(\bar{t})\chi_b(\bar{t})$$

$$=-\frac{1}{4}\sum_n e^{-in\omega t}\sum_b \int_0^{t-t_0} d\tau I_{ab}^{(2)}(n;t,\tau), \quad \text{(A1)}$$

with

$$I_{ab}^{(2)}(n;t,\tau) = D_{ab}^{(2)}(\tau) \times (E(t)E(t-\tau)e^{i(n-1)\omega\tau}\chi_b(n-2;t-\tau)$$
$$+ E(t)E^*(t-\tau)e^{i(n-1)\omega\tau}\chi_b(n;t-\tau)$$
$$+ E^*(t)E(t-\tau)e^{i(n+1)\omega\tau}\chi_b(n;t-\tau)$$
$$+ E^*(t)E^*(t-\tau)e^{i(n+1)\omega\tau}\chi_b(n+2;t-\tau)). \quad \text{(A2)}$$

As underlined in Sec. IV the RWA reduces the set of functions $\chi_a(n;t)$ to $\chi_g(0;t)$ and $\chi_e(2;t)$. At the same time the set of $I_{ab}^{(2)}(n;t,\tau)$ has to be specified, respectively.

Since the expansion functions, as well as the field envelopes, vary slowly in time compared to the carrier wave oscillations, we may take them out of the τ integral applied to the various $I_{ab}^{(2)}$. Then, time integrals with respect to $D_{ab}^{(2)}(\tau)$ remain. In order to calculate them we introduce the DOS of the secondary states resulting in

$$D_{ab}^{(2)}(\tau) = \frac{i}{\hbar} \int d\Omega \varrho(\Omega) d(a,\Omega) e^{-i\Omega\tau} d(\Omega,b), \qquad (A3)$$

where $d(a,\Omega)$ and $d(\Omega,b)$ couple the primary states φ_a and φ_b, respectively, to the manifold of secondary states. Noting Eq. (A3), as well as $t_0 \to -\infty$ and $\nu = \pm 1, 3$, we introduce the effective (two-photon) coupling matrix element

$$d_{ab}^{(2)} = \int_0^\infty d\tau e^{i\nu\omega\tau} D_{ab}^{(2)}(\tau) =$$

$$-\frac{1}{\hbar} \int d\Omega \varrho(\Omega) \frac{d(a,\Omega)d(\Omega,b)}{\nu\omega - \Omega + i\epsilon}. \qquad (A4)$$

If $\nu\omega \lesssim 3\omega$ is much smaller than the range where the secondary state frequencies Ω start to contribute, we may write

$$d_{ab}^{(2)} \approx \frac{1}{\hbar} \int \frac{d\Omega}{\Omega} \varrho(\Omega) d(a,\Omega) d(\Omega,b) \approx \frac{\bar{\varrho}}{\hbar} d_{\text{eff}}^2. \qquad (A5)$$

Of course, replacing $d_{ab}^{(2)}$ by a mean value $\bar{\varrho}$ of the DOS and the square of an effective transition dipole moment d_{eff}, as

done in the last step of our calculations, seems to be a rather crude approximation. Nevertheless it offers a suitable parametrization for those cases where no other possibility exists to get access to more precise values.

The three-photon term of Eq. (16) is reformulated in the same way as the two-photon one. We introduce $D_{ab}^{(3)} = \mathbf{D}_{ab}^{(3)}\mathbf{nnn}$ (a third-rank tensor multiplied by three ordinary unit vectors) and change to new time arguments $t - \bar{t} = \tau$ and $t_1 - \bar{t} = \bar{\tau}$. The index n is replaced in such a way to have a common prefactor $\exp(-in\omega t)$ for all terms. This results in

$$-\sum_b \int_{t_0}^t d\bar{t} \int_{\bar{t}}^t dt_1 \mathbf{D}_{ab}^{(3)}(t - t_1, t_1 - \bar{t}) \mathbf{E}(t)\mathbf{E}(t_1)\mathbf{E}(\bar{t})\chi_b(\bar{t})$$

$$= -\frac{1}{8}\sum_n e^{-in\omega t} \sum_b \int_0^{t-t_0} d\tau \int_0^\tau d\bar{\tau} I_{ab}^{(3)}(n;t,\tau,\bar{\tau}), \qquad (A6)$$

with

$$I_{ab}^{(3)}(n;t,\tau,\bar{\tau}) = D_{ab}^{(3)}(\tau - \bar{\tau}, \bar{\tau})(E(t)E(t-(\tau-\bar{\tau}))E(t-\tau)e^{-i\omega\bar{\tau}+i(n-1)\omega\tau}\chi_b(n-3;t-\tau) + E(t)E^*(t-(\tau-\bar{\tau}))$$

$$\times E(t-\tau)e^{i\omega\bar{\tau}+i(n-1)\omega\tau}\chi_b(n-1;t-\tau) + E^*(t)E(t-(\tau-\bar{\tau}))E(t-\tau)e^{-i\omega\bar{\tau}+i(n+1)\omega\tau}\chi_b(n-1;t-\tau)$$

$$+ E^*(t)E^*(t-(\tau-\bar{\tau}))E(t-\tau)e^{i\omega\bar{\tau}+i(n+1)\omega\tau}\chi_b(n+1;t-\tau) + E(t)E(t-(\tau-\bar{\tau}))E^*(t-\tau)e^{-i\omega\bar{\tau}+i(n-1)\omega\tau}$$

$$\times \chi_b(n-1;t-\tau) + E(t)E^*(t-(\tau-\bar{\tau}))E^*(t-\tau)e^{i\omega\bar{\tau}+i(n+1)\omega\tau}\chi_b(n+1;t-\tau) + E^*(t)E(t-(\tau-\bar{\tau}))$$

$$\times E^*(t-\tau)e^{-i\omega\bar{\tau}+i(n+1)\omega\tau}\chi_b(n+1;t-\tau) + E^*(t)E^*(t-(\tau-\bar{\tau}))E^*(t-\tau)e^{i\omega\bar{\tau}+i(n+1)\omega\tau}\chi_b(n+3;t-\tau)). \qquad (A7)$$

The RWA reduces the set of functions $\chi_a(n;t)$ to $\chi_g(0;t)$ and $\chi_e(3;t)$, and the $I_{ab}^{(3)}(n;t,\tau,\bar{\tau})$ turn into the following nonvanishing expressions:

$$I_{ge}^{(3)}(0;t,\tau,\bar{\tau}) = D_{ge}^{(3)}(\tau - \bar{\tau}, \bar{\tau})E^*(t)E^*(t-(\tau-\bar{\tau}))$$

$$\times E^*(t-\tau)e^{i\omega\bar{\tau}+i\omega\tau}\chi_e(3;t-\tau). \qquad (A8)$$

and

$$I_{eg}^{(3)}(3;t,\tau,\bar{\tau}) = D_{eg}^{(3)}(\tau - \bar{\tau}, \bar{\tau})E(t)E(t-(\tau-\bar{\tau}))$$

$$\times E(t-\tau)e^{-i\omega\bar{\tau}-2i\omega\tau}\chi_g(0;t-\tau). \qquad (A9)$$

As in the foregoing section, the application of the SVA results in products of field envelopes and the expansion function at time argumet t. A double time integral with respect to $D_{ge}^{(3)}$ and $D_{eg}^{(3)}$ remains. We first take into consideration $(a,b = g,e)$

$$D_{ab}^{(3)}(\tau - \bar{\tau}, \bar{\tau}) = \frac{1}{\hbar^2} \int d\Omega d\bar{\Omega} \varrho(\Omega) \varrho(\bar{\Omega})$$

$$\times d(a,\Omega) e^{-i\Omega(\tau-\bar{\tau})} d(\Omega,\bar{\Omega}) e^{-i\bar{\Omega}\bar{\tau}} d(\bar{\Omega},b). \qquad (A10)$$

Setting $t_0 \to -\infty$ and noting $\mu = \pm 1$ and $\nu = 1, -2$, the effective

(three-photon) coupling matrix element can be defined as

$$d_{ab}^{(3)} = \int_0^\infty d\tau \int_0^\tau d\bar{\tau} D_{ab}^{(3)}(\tau - \bar{\tau}, \bar{\tau}) e^{i\mu\omega\tau + i\nu\omega\bar{\tau}}$$

$$= -\frac{1}{\hbar^2} \int_0^\infty d\tau \int_0^\tau d\bar{\tau} \int d\Omega d\bar{\Omega} \varrho(\Omega)\varrho(\bar{\Omega})$$

$$\times e^{i(\mu\omega-\Omega)\tau + i(\nu\omega+\Omega-\bar{\Omega})\bar{\tau}} d(a,\Omega)d(\Omega,\bar{\Omega})d(\bar{\Omega},b)$$

$$= -\frac{1}{\hbar^2} \int d\Omega d\bar{\Omega} \frac{\varrho(\Omega)\varrho(\bar{\Omega})d(a,\Omega)d(\Omega,\bar{\Omega})d(\bar{\Omega},b)}{\nu\omega + \Omega - \bar{\Omega}}$$

$$\times \left(\frac{1}{(\mu+\nu)\omega - \bar{\Omega} + i\epsilon} - \frac{1}{\mu\omega - \Omega + i\epsilon} \right). \qquad (A11)$$

Again $(\mu+\nu)\omega$ should be much smaller than the range where the secondary state frequencies Ω and $\bar{\Omega}$ start to contribute. Then, the following approximations can be taken:

$$d_{ab}^{(3)} \approx \frac{1}{\hbar^2} \int d\Omega d\bar{\Omega} \varrho(\Omega) \varrho(\bar{\Omega}) d(a,\Omega) d(\Omega,\bar{\Omega}) d(\bar{\Omega},b)$$

$$\times \frac{\Omega - \bar{\Omega}}{(\Omega - \bar{\Omega})\Omega\bar{\Omega}}$$

$$\approx \frac{1}{\hbar^2} \int d\Omega \frac{\varrho(\Omega) d(a,\Omega)}{\Omega} \int d\bar{\Omega} \frac{\varrho(\bar{\Omega}) d(\Omega,\bar{\Omega}) d(\bar{\Omega},b)}{\bar{\Omega}}$$

$$\approx \frac{\bar{\varrho}^2}{\hbar^2} d_{\text{eff}}^3. \tag{A12}$$

Similar to the two-photon case this expression provides a suitable parametrization of the effective coupling matrix element.

[1] F. H. M. Faisal, *Theory of Multiphoton Processes* (Plenum, New York, 1987).
[2] L. Frediani, Z. Rinkevicius, and H. Ågren, J. Chem. Phys. **122**, 244104 (2005).
[3] S.-I. Chu, J. Chem. Phys. **123**, 062207 (2005).
[4] M. J. Paterson, O. Christiansen, F. Pawlowski, P. Jorgensen, Ch. Hätting, T. Helgaker, and P. Salek, J. Chem. Phys. **124**, 054322 (2006).
[5] P. N. Day, K. A. Nguyen, and R. Pachter, J. Chem. Phys. **125**, 094103 (2006).
[6] D. Meshulach and Y. Silberberg, Nature (London) **396**, 239 (1998).
[7] D. Meshulach and Y. Silberberg, Phys. Rev. A **60**, 1287 (1999).
[8] K. A. Walowicz, I. Pastirk, V. V. Lozovoz, and M. Dantus, J. Phys. Chem. A **106**, 9369 (2002).
[9] V. V. Lozovoy, I. Pastirk, K. A. Walowicz, and M. Dantus, J. Chem. Phys. **118**, 3187 (2003).
[10] C. Daniel, J. Full, L. González, C. Lupulescu, J. Manz, A. Merli, S. Vajda, and L. Wöste, Science **299**, 536 (2003).
[11] S. A. Rice and M. Zhao, *Optical Control of Molecular Dynamics* (Wiley, New York, 2000).
[12] M. Shapiro and P. Brumer, *Principles of the Quantum Control of Molecular Processes* (Wiley, Hoboken, NJ, 2003).
[13] V. May and O. Kühn, *Charge and Energy Transfer Dynamics in Molecular Systems*, 2nd ed. (Wiley-VCH, Weinheim, 2004).
[14] *Coherent Control of Photochemical and Photobiological Processes*, edited by J. L. Herek, special issue of J. Photochem. Photobiol., A **180**, 225 (2006).
[15] *Quantum Control of Light and Matter*, edited by Th. Halfmann, special issue of Opt. Commun. **264**, 247 (2006).
[16] Proceedings of the CCP6 workshop on Coherent Control of Molecules, Daresbury, UK, 2006, edited by B. Lasorne and G. A. Worth.
[17] *Analysis and Control of Photoinduced Ultrafast Reactions*, Springer Series in Chemical Physics Springer Vol. 87, edited by O. Kühn and L. Wöste (Springer-Verlag, Berlin, 2007).
[18] D. Ambrosek, M. Oppel, L. González, and V. May, Chem. Phys. Lett. **380**, 536 (2003).
[19] D. Ambrosek, M. Oppel, L. González, and V. May, *Quantum Control of Light and Matter*, edited by Th. Holfmann, special issue of Opt. Commun. **264**, 502 (2006).
[20] T. Kreibich, M. Lein, V. Engel, and E. K. U. Gross, Phys. Rev. Lett. **87**, 103901 (2001).
[21] M. Lein, N. Hay, R. Velotta, J. P. Marangos, and P. L. Knight, Phys. Rev. Lett. **88**, 183903 (2002).
[22] M. Erdmann, P. Marquetand, and V. Engel, J. Chem. Phys. **119**, 672 (2003).
[23] M. Erdmann and V. Engel, J. Chem. Phys. **120**, 158 (2004).
[24] R. Xu, J. Cheng, and Y. J. Yan, J. Phys. Chem. A **103**, 10611 (1999).
[25] S. A Hosseini and D. Goswami, Phys. Rev. A **64**, 033410 (2001).
[26] A. P. Pierce, M. A. Dahleh, and H. Rabitz, Phys. Rev. A **37**, 4950 (1988).
[27] S. Shi, A. Woody, and H. Rabitz, J. Chem. Phys. **88**, 6870 (1988).
[28] Y. J. Yan, R. E. Gillian, R. M. Whitnell, K. R. Wilson, and S. Mukamel, J. Phys. Chem. **97**, 2320 (1993).
[29] W. Zhu, J. Botina, and H. Rabitz, J. Chem. Phys. **108**, 1953 (1998).
[30] W. Zhu and H. Rabitz, J. Chem. Phys. **109**, 385 (1998).
[31] Y. Ohtsuki, W. Zhu, and H. Rabitz, J. Chem. Phys. **110**, 9825 (1999).
[32] J. Full, C. Daniel, and L. González, Phys. Chem. Chem. Phys. **5**, 87 (2003).
[33] L. González and J. Full, Theor. Chem. Acc. **116**, 148 (2006).